

Article

A New Nephrite Occurrence in Jiangxi Province, China: Its Characterization and Gemological Significance

Xin Wei ¹, Guanghai Shi ^{1,*} , Xiaochong Zhang ^{1,2}, Jiajing Zhang ³ and Meiyu Shih ¹ ¹ School of Gemmology, China University of Geosciences (Beijing), Beijing 100083, China² School of Management, Tianjin University of Commerce, Tianjin 300134, China³ Jiangxi College of Applied Technology, Ganzhou 341000, China

* Correspondence: shigh@cugb.edu.cn

Abstract: Nephrite is a very precious gemstone material. As a non-renewable resource, the discovery of new nephrite deposits and the study of the genesis of nephrite have aroused great interest. A new occurrence of nephrite known as Xinyu nephrite was discovered in Xinyu Country, Jiangxi province, China. Field investigations reveal that nephrite appears in a contact zone between the Mengshan composite granitic pluton and Permian carbonate rock. The carbonate rock is calcic marble that underwent diopsidization and tremolitization. Nephrites have a light yellow-green color, weak greasy luster, are slightly-translucent to translucent, and are fine-grained. Their refractive index (RI) ranges from 1.60 to 1.61, and their specific gravity (SG) value ranges from 2.90 to 2.91, falling within the range of nephrites from Xinjiang, China. Their Mohs hardness (Hm) ranges from 5.78 to 5.83. Petrographic observations and electron probe micro analyzer (EPMA) data indicated that analyzed nephrites mainly comprise tremolite, with minor diopside, calcite, quartz, and apatite. Tremolite has a ratio of Mg/(Mg + Fe²⁺) greater than 0.99. The tremolite grains show microscopic fibrous-felted and columnar textures. Scanning electron microscope (SEM) images show some tremolite fibers interwoven in different crystallographic orientations, and some arranged in parallel. Fourier transform infrared and Raman spectroscopy features reveal the bands of minerals typical for nephrite composition. The petrographic characteristics and geological background of the Mengshan area indicate that nephrite formed through a replacement of calcic marble, which differs from the two known types (D-type: dolomite-related; S-type: serpentinite-related). Mineral replacements were common in nephrite, including diopside by tremolite, calcite by tremolite, and recrystallization of coarse by fine tremolite grains. The discovery of Xinyu nephrite occurrence complements the resource and provides an updated case for the in-depth study of the diversity of nephrite deposits.

Keywords: Xinyu nephrite; tremolite; diopside; genesis; Mengshan area



Citation: Wei, X.; Shi, G.; Zhang, X.; Zhang, J.; Shih, M. A New Nephrite Occurrence in Jiangxi Province, China: Its Characterization and Gemological Significance. *Minerals* **2024**, *14*, 432. <https://doi.org/10.3390/min14040432>

Academic Editor: Frederick Lin Sutherland

Received: 7 March 2024

Revised: 10 April 2024

Accepted: 19 April 2024

Published: 21 April 2024



Copyright: © 2024 by the authors. Licensee MDPI, Basel, Switzerland. This article is an open access article distributed under the terms and conditions of the Creative Commons Attribution (CC BY) license (<https://creativecommons.org/licenses/by/4.0/>).

1. Introduction

Tremolite jade, known as nephrite, is an important jade species used in jewelry since ancient eras [1], captivating people worldwide. Nephrite primarily consists of tremolite-actinolite [Ca₂(Mg, Fe)₅[Si₄O₁₁]₂(OH)₂] minerals of the hornblende group, and often contains calcite, diopside, quartz, apatite, chlorite, epidote, or other minor minerals [2].

Nephrite deposits are common worldwide, such as in China [3], Russia [4], Korea [5,6], Canada [7,8], and Somaliland in Africa [9], which has important economic implications. In China, the culture of nephrite has a long history [10,11], and the origin of nephrite is widely distributed, such as in Xinjiang [12–14], Qinghai [15,16], Dahua, Guangxi [17], Xiuyan, Liaoning [18,19], Panshi, Jilin [20], Tieli, Heilongjiang [21], etc.

Although nephrites have been reported to be found around the world, resources are slowly diminishing due to the constant advances in modern mining technology and increasing demand. The discovery of new sources is extremely important in augmenting global nephrite reserves.

Jiangxi province has significant non-metallic mineral resources, such as diopside [22], and wollastonite with world-class reserves [23]. However, there have been no reports on the geology of nephrite deposits in the province. Previous studies have identified tremolite existing in the non-metallic deposits as a minor mineral, with no reports of tremolite aggregates, or even gem-quality nephrites.

This paper studies the discovery of a gem-quality nephrite jade occurrence from Xinyu County, Jiangxi Province. We provide comprehensive data on the gemological, mineralogical, geochemical, and spectral characteristics of Xinyu nephrite, in order to explore its formation process and its potential resource as a jewelry material.

2. Geological Setting

2.1. Regional Geology

New nephrites reported in this study were collected in the Mengshan area (GPS: $114^{\circ}54'–57'$ E, $28^{\circ}02'–05'$ N) of Xinyu County, Jiangxi Province. This area is located in the eastern segment of the Qinhang Metallogenic belt, which was formed by the collision and splicing of the two ancient continents, namely the Yangtze and Cathaysia blocks, during the middle and advanced stage (Figure 1) [24].

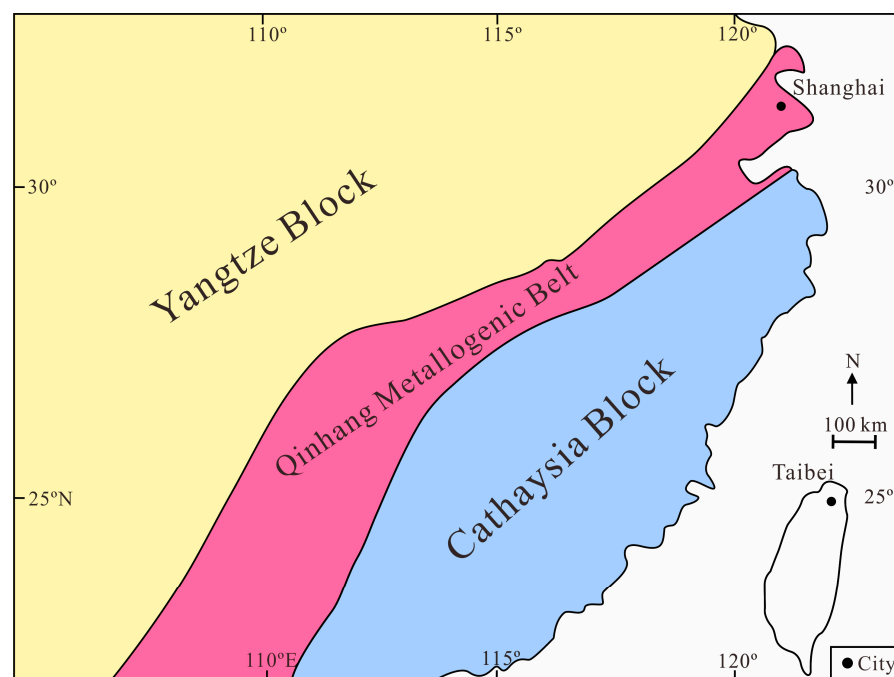


Figure 1. The geological background of the Mengshan area is located in the eastern segment of the Qinhang Metallogenic belt (modified after [25]).

The strata exposed in the Mengshan and surrounding areas are Carboniferous to Triassic. Among them, the Carboniferous Huanglong Formation, Permian Qixia Formation, Permian Leping Formation, and Permian Maokou Formation form a set of carbonate rock associations. These formations primarily consist of limestone, dolomitic limestone, dolomite, and carbonaceous rock (Figure 2) [26]. The Mengshan area has favorable conditions for mineralization. The abundance values of tungsten, copper, zinc, molybdenum, tin, and other metallogenic elements in the formation are higher than those of crustal elements in the eastern part of China [27]. Therefore, the surroundings of the Mengshan granite pluton are prone to metasomatism or hydrothermal metamorphism, leading to the dense distribution of skarn-type deposits in the area [23,28,29].

The rock folds and faults in the Mengshan area are developed, and the tectonic lines indicate an overall north-eastward spreading, followed by near east-west, north-east, and north-westward. In particular, folds or fractures in the Carboniferous-Permian strata are

highly susceptible to fragmentation or interlayer slip by late extrusion. This phenomenon helps to promote the transport and enrichment of mineralized elements [23].

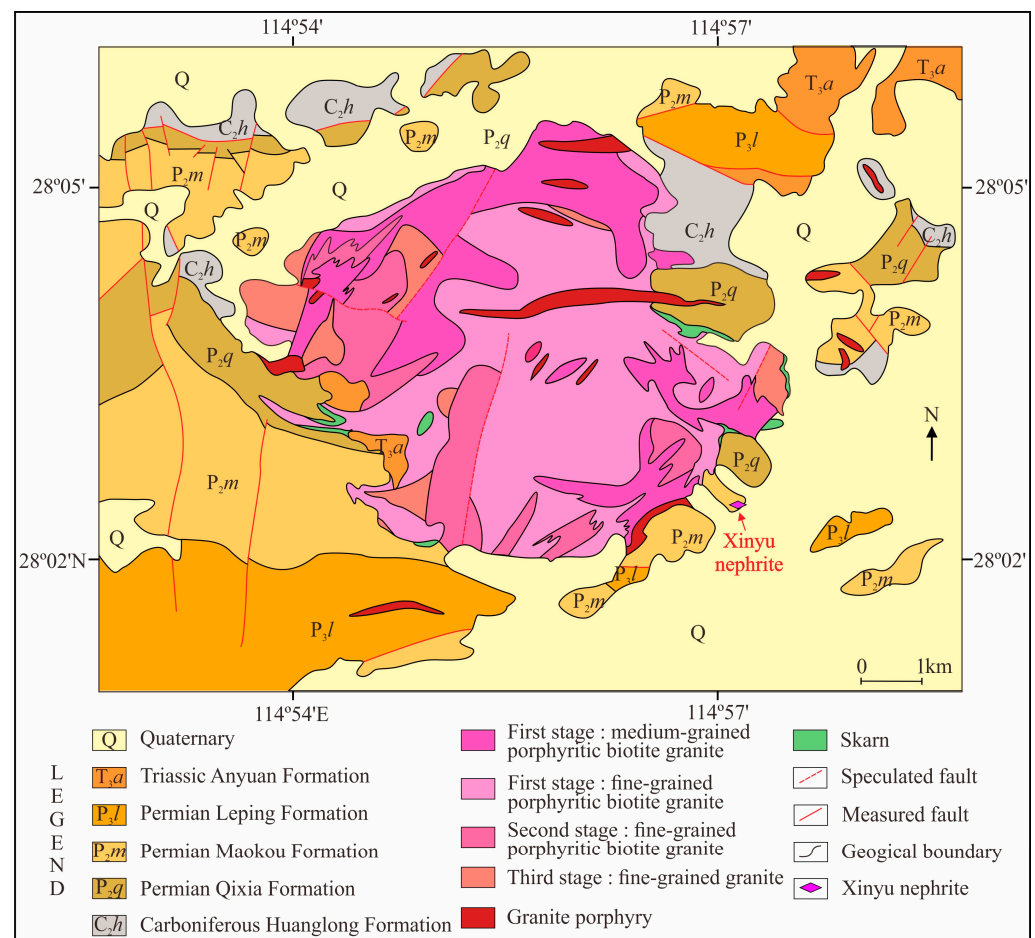


Figure 2. Geological map of the Mengshan area. The Mengshan composite pluton and surrounding exposed strata (modified after [23]).

2.2. The Mengshan Composite Pluton

Influenced by the tectonic events of the Triassic and Jurassic-Cretaceous, the Mengshan area underwent multiple phases of magmatism resulting in the formation of the Mengshan composite pluton was formed as a result [30,31], which covers an area of about 39 km² [28].

The Mengshan composite pluton consists of Triassic granites (~217 to ~236 Ma) [28] and Jurassic-Cretaceous dikes (~135 Ma and ~142 Ma) [26,28]. Previous studies [26] divided the Mengshan Triassic granites into three stages. The first-stage granites constitute the main body (71%) and can be further subdivided into two phases: the transitional and marginal phases. The transitional phase consists of medium-grained porphyritic biotite granite, while the marginal phase consists of fine-grained biotite granite. The second-stage granites are composed of fine-grained porphyritic biotite granite, and the third stage is composed of fine-grained granite. Jurassic-Cretaceous igneous rocks, in the form of veins and dikes, intruded into the Triassic granites and surrounding sedimentary rocks. These vein rocks mainly consist of granite porphyry and diorite porphyry.

According to the geological background of the Mengshan area mentioned earlier, it can be concluded that the tectonic conditions create a favorable environment for mineralization, and the complex magmatic activity supplies mineral-bearing hydrothermal fluids for contact metasomatism. These factors collectively provide advantageous conditions for the mineralization of skarn-type tremolite, diopside, wollastonite, etc.

2.3. Location of Xinyu Nephrite Occurrence

Xinyu nephrite occurs in the southeastern part of the Mengshan composite pluton, located in the contact zone of the Permian Maokou Formation with the pluton (Figure 2). Geological information shows that the lower part of the Permian Maokou Formation is cryptocrystalline limestone, calcareous limestone interbedded with muddy limestone, and the upper part is dark grey cryptocrystalline structural limestone interbedded with calcareous mudstone.

3. Samples and Methods

3.1. Samples

In this study, two samples from Xinyu County, Jiangxi Province, were collected and studied (Figure 3a,b). Polished thin sections (0.25 mm) were made for petrographic observation and compositional analysis. Thick nephrite polished plates (5 mm) (Figure 3c,d) were also used for conventional gemological testing and quality evaluation. The new nephrite jades have a light yellow-green color, showing dense textures and a blocky structure.

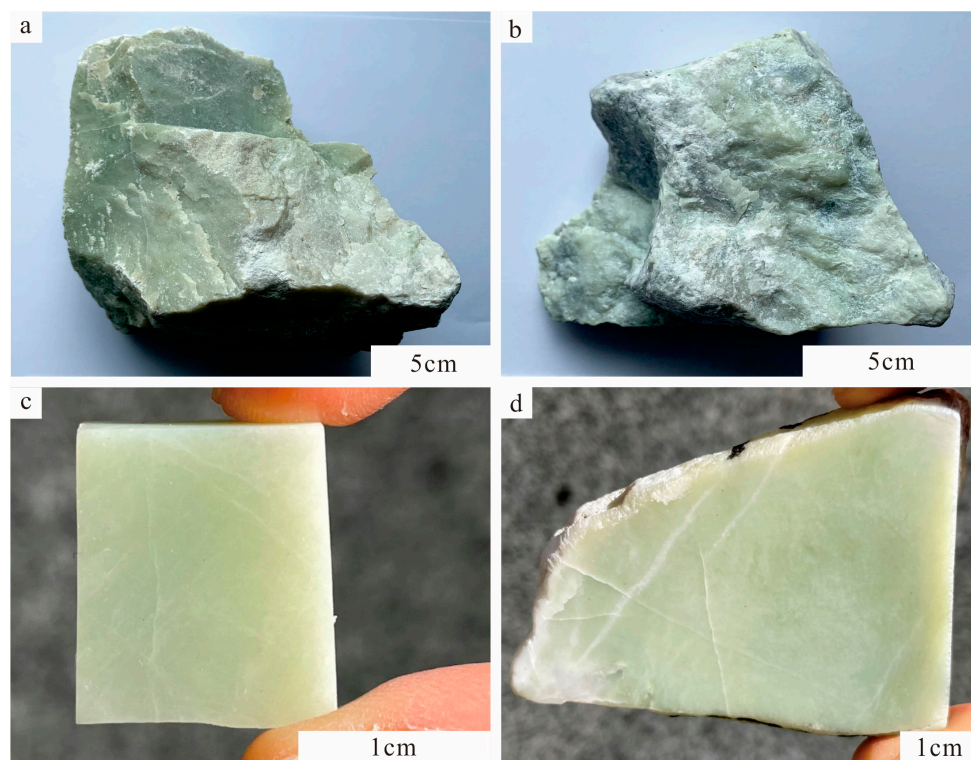


Figure 3. Photograph of the samples collected in Xinyu County, Jiangxi Province. (a) Tough nephrite sample. It has a light green color, slightly translucent, and fine texture. (b) Tough nephrite sample. It has a light green color, slightly translucent, and the texture is a little rougher than that of (a). (c,d) Polished nephrite jade plates were made from the samples collected in Xinyu.

3.2. Analytical Methods

Gemological characteristic tests were conducted at the Gemological Experimental Teaching Center of China University of Geosciences, Beijing (CUGB). The reflection index (RI) was measured using the GR-6 refractometer by spot measurements. The specific gravity (SG) was measured using a high-precision electronic scale using hydrostatic weighing. Mohs hardness (Hm) was measured using the TH763 digital display microhardness tester, employing the indentation method. Vickers hardness of the measured points was obtained from the indentation test, and the formula “Vickers hardness (HV) = 3.25 × (Mohs hardness) 3 (Hm)” was applied to convert the date. To eliminate the accidental error, each of the

above tests was conducted three times and then their average value was taken as the reported result.

Petrographic characteristics were observed at the Gemological Experimental Teaching Center, CUGB. Polished thin sections of the samples were observed using an OLYMPUS BX5 polarizing microscope to determine mineral assemblage microtexture characteristics and contact relationships of minerals under transmitted light.

Chemical composition and backscattered electron (BSE) images were obtained at the Electron Probe Laboratory of the Institute of Science, CUGB, using a Shimadzu EPMA-1600 Electron Probe Microprobe Analyzer (EPMA). Before analysis, samples were coated with a thin conductive carbon film, approximately 20 nm in thickness. During analysis, the minerals were analyzed using a beam spot with an accelerating voltage of 15 kV, a current of 7 nA, and a diameter of 1 μm . Natural minerals and synthetic oxides were used as standards. Data were corrected online using a modified ZAF (atomic number, absorption, fluorescence) correction procedure.

The spectroscopic characterization study included Fourier transform infrared spectroscopy (FTIR) and Laser Raman spectroscopy, both obtained at the Gemological Experimental Teaching Center of CUGB. FTIR features were obtained using a BrukerTensor27 Fourier transform infrared spectrometer with a scan range of 2000–200 cm^{-1} and resolution of 4 cm^{-1} . A total of 32 scans were performed at ~ 20 $^{\circ}\text{C}$ for both the sample and the background. Testing was performed on a single polished slice using the reflection method. Laser Raman characterization was performed using a LabRAM HR Evolution micro-Raman spectroscopy. Experimental settings included a laser emission wavelength of 532 nm, laser power ranging from 30 mW to 40 mW, a spectral resolution of ≤ 0.35 cm^{-1} , a scan time of 20 s, and a test range of 100–2000 cm^{-1} .

Microtexture features were obtained at the Scanning Electron Microscope Laboratory of the Institute of Science, CUGB, using a ZEISS SUPRA55 field emission scanning electron microscope (SEM). After platinum spray treatment, thick polished plates (5 mm) were analyzed at an accelerating voltage of 10 kV at ~ 20 $^{\circ}\text{C}$.

All the research contents and instruments in this research are listed in Table 1.

Table 1. Description of the research contents and instruments in this research.

Research Content	Measurement Unit	Instrument
Gemological characteristic tests	Gemological Experimental Teaching Center, CUGB	Reflection index: GR-6 Refractometer
		Specific gravity: High-precision electronic scale
		Mohs hardness: TH763 digital display microhardness tester
Petrographic characteristics	Gemological Experimental Teaching Center, CUGB	OLYMPUS BX5 polarizing microscope
Chemical composition and backscattered electron images	Electron Probe Laboratory of the Institute of Science, CUGB	Shimadzu EPMA-1600 Electron Probe Microprobe Analyzer
Spectroscopic characterization	Gemological Experimental Teaching Center, CUGB	BrukerTensor27 Fourier transform infrared spectrometer
		LabRAM HR-Evolution micro-Raman spectroscopy
Microtexture features	Scanning Electron Microscope Laboratory of the Institute of Science, CUGB	Zeiss SUPRA55 field emission scanning electron microscope

4. Results

4.1. Gemological Properties

Xinyu nephrite jades are mostly slightly-translucent to translucent in light yellow-green. No white, black, or vivid green type of jade has been found so far.

Nephrites have a medium-greasy luster and show homogeneous, compact, and fine textures (Figure 3c,d). Near the surface, there are some whitish substances in the form of fine lines (Figure 3c,d). Accurate gemological tests yield a reflection index (RI) of 1.60–1.61, specific gravity (SG) of 2.90–2.91, and Mohs hardness (Hm) of 5.78–5.83 (Table 2). The RI and SG values are within the range of gemological tests for nephrites from Xinjiang, China [32], but the Hm value is slightly lower. There are no fluorescence characteristics under the ultraviolet fluorescent lamp and no significant spectrum under the grid spectroscope. SEM imaging showed that tremolite grains in jade occur as long fibers, which are ~30 μm in length and 0.1–0.2 μm in diameter (Figure 4). Some of the fibers are interwoven in different crystallographic orientations, and some are arranged in parallel. The jades are therefore thought to be fine and tough and could be defined as gem-quality based on their appearance and textural characteristics.

Table 2. Gemological Properties of Xinyu Nephrite.

Name	Characteristic
Color	Light yellow-green
Luster	Medium-greasy
Transparency	Slightly-translucent to translucent
Refractive Index	1.60–1.61
Specific Gravity	2.90–2.91
Mohs Hardness	5.78–5.83

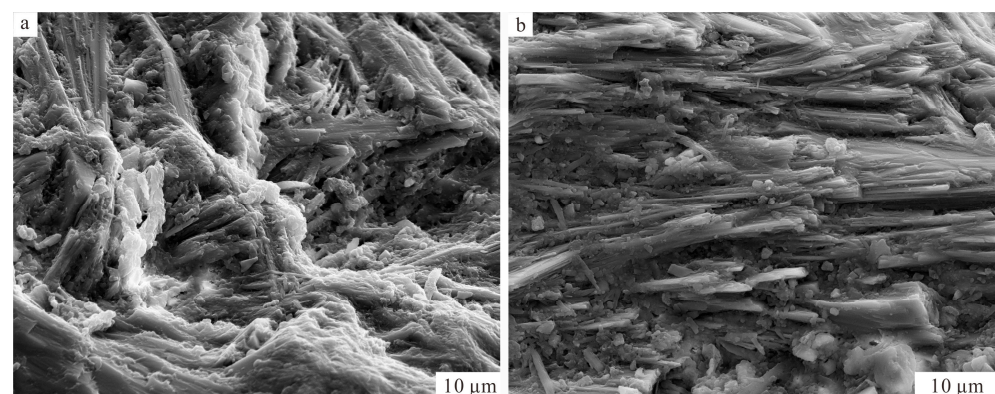


Figure 4. SEM imaging of Xinyu nephrite. (a) Fibrous tremolites are interwoven in different crystallographic orientations. (b) Long fibrous tremolites arranged in parallel.

4.2. Petrographic Characteristics

4.2.1. Xinyu Nephrite

The nephrite from Xinyu comprises predominantly tremolite (Tr: >98 vol.%), with other minor minerals including diopside, calcite, quartz, and apatite.

In the samples, two types of tremolite grains were observed. The first type of grains appeared as microscopic fibrous-felted textures (Figure 5a). Most of these grains were straight and dense, in a directional parallel arrangement. The outlines and shapes are not distinguishable, but the grains are tightly bound and evenly distributed. These types of grains are commonly observed, which is probably the main factor determining the fine and smooth macroscopic appearance of Xinyu nephrite. The second grains appeared as coarse, columnar textures (Figure 5b) which are ~500 μm in length and ~115 μm in width. The core of the coarse grains was often replaced by fine tremolite grains, and the incomplete replacements resulted in the shape of the original coarse grains being retained.

Fibrous tremolites can be observed at the grain boundaries of other minerals, such as diopside (Figure 5c) and calcite (Figure 5d), indicating frequent replacement of minerals by tremolite. The tremolite that replaced the diopside is microscopically crypto-crystalline and fibrous, with a poorly defined, fibrous-felted texture between grains (Figure 5c). As the

grain sizes are all relatively small, no obvious mineral–mineral interspersed relationships are observed. Diopside occurs as discrete rounded grains surrounded by fibrous tremolite in an isolated, island-like form (Figure 5e,f).

Texture of tremolite replacing calcite often occurs, and replaced calcite grains show replacement residual structures (Figure 5d). Apatite grains are extremely small and scattered in the samples (Figure 5f).

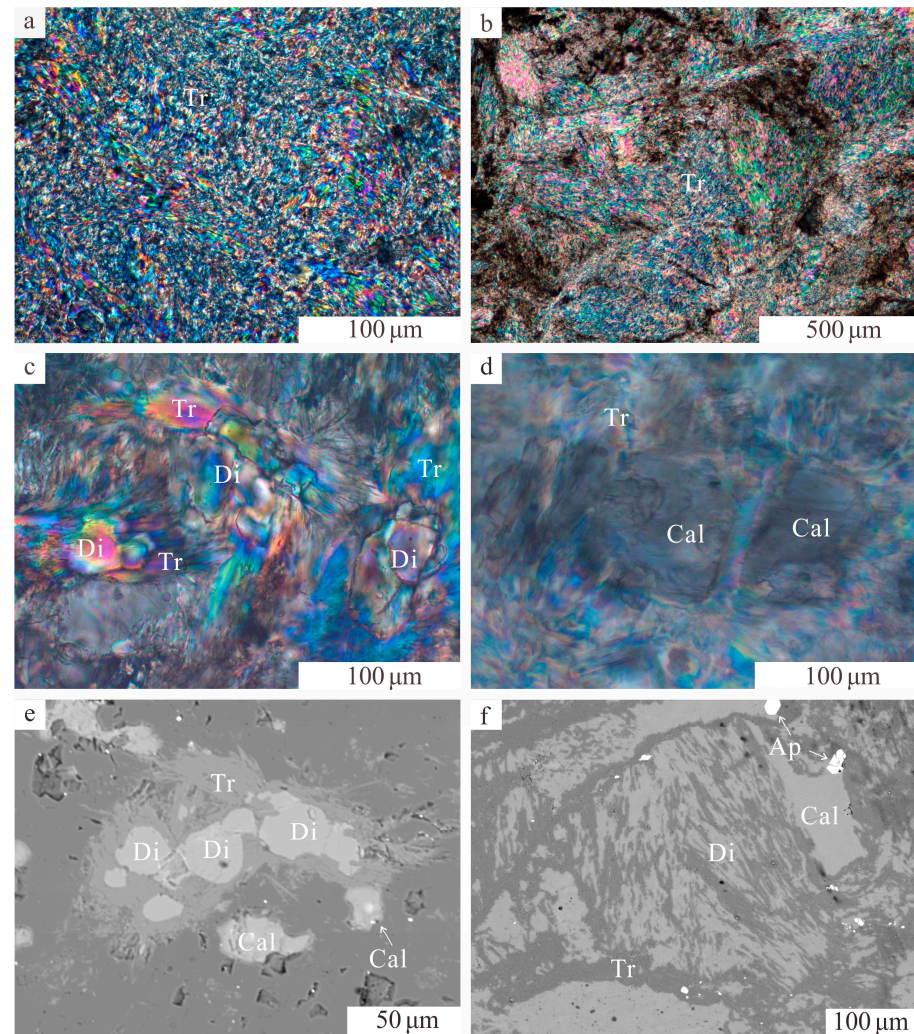


Figure 5. Polarized light microphotographs (a–d) and BSE images (e,f) of Xinyu nephrite. (a) The tremolite grains are fibrous and felted. (b) The tremolite grains are coarse and columnar. (c) Diopside was replaced by tremolite. (d) Calcite was replaced by tremolite, leaving remnants of the calcite. (e) A BSE image shows an isolated island diopside being replaced by tremolite. (f) A BSE image of diopside being replaced by tremolite resulting in hardly intact diopside grains. Apatite can be seen. (Tr—tremolite; Di—diopside; Cal—calcite; Ap—apatite).

4.2.2. The Carbonate Rock

The carbonate rock is calcic marble that mainly underwent diopsidization and tremolization (Figure 6a,b). It has a granular texture, and the component minerals are tightly packed without preferential orientation. Some calcite grains are replaced by fibrous tremolites. Diopside grains can also be seen. A clear transition between the tremolite zone and the marble zone can be seen in Figure 6c,d. However, this contact line is not straight, and the minerals close to the line are closely intertwined.

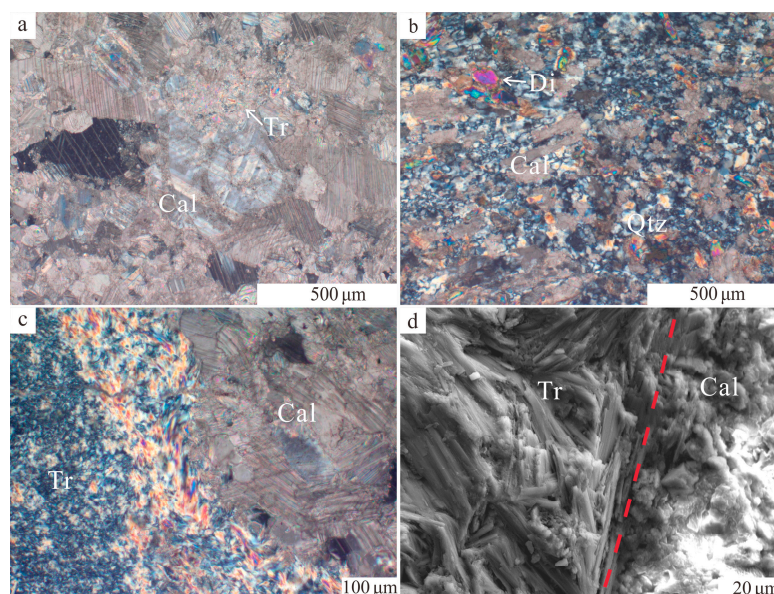


Figure 6. Polarized light microphotographs (a–c) and BSE images (d) of Carbonate rock. (a,b) Structural characteristics of carbonate rock (underwent diopsidization and tremolitization calcic marble). Fibrous tremolite can be seen between some of the tightly arranged calcite grains. Diopside grains are locally visible. (c,d) Clear contact transition between tremolite and calcite. The red dashed line indicates the clear boundary between tremolite and calcite, both of them are tightly intertwined. (Tr—tremolite; Di—diopside; Cal—calcite; Qtz—quartz).

4.3. Mineral Chemistry

According to calculated ratios of $Mg/(Mg + Fe^{2+})$, all amphiboles in Xinyu nephrite are classified as tremolite (Table 3) (Figure 7) [33]. Tremolite is mainly composed of (in wt.%) SiO_2 (57.86–59.02), CaO (12.29–12.67), and MgO (24.88–25.57). The atoms per formula unit (a.p.f.u.) values for tremolite are as follows: $Si = 7.91$ – 7.98 , Ca on B site = 1.76 – 1.85 , $(Na + K)$ on A site ≤ 0.05 . The $Mg/(Mg + Fe^{2+})$ ratio for tremolite is greater than 0.99.

Table 3. Chemical composition of tremolite in the Xinyu nephrite (wt.%).

Samples	XY-2	XY-2	XY-3	XY-3	XY-3
No.	1	2	6	7	8
SiO_2	57.86	58.18	58.59	58.40	59.02
TiO_2	0.00	0.03	0.01	0.00	0.00
V_2O_5	0.02	0.00	0.00	0.00	0.00
Al_2O_3	0.23	0.36	0.27	0.22	0.33
Cr_2O_3	0.00	0.03	0.02	0.00	0.04
FeO	0.21	0.25	0.26	0.26	0.42
MgO	25.57	25.41	24.95	24.88	24.90
MnO	0.01	0.02	0.05	0.02	0.04
NiO	0.00	0.06	0.03	0.03	0.01
ZnO	0.11	0.00	0.00	0.00	0.00
CaO	12.67	12.29	12.63	12.64	12.37
CoO	0.00	0.00	0.01	0.00	0.00
Na_2O	0.09	0.15	0.06	0.07	0.10
K_2O	0.01	0.06	0.06	0.03	0.06
SO_3	0.00	0.01	0.00	0.00	0.00
P_2O_5	0.00	0.00	0.01	0.01	0.02
F	0.00	0.00	0.38	0.30	0.33
Total	96.78	96.84	97.16	96.74	97.48
H_2O_{calc}	2.19	2.20	2.03	2.06	2.06
Total _{calc}	98.97	99.04	99.19	98.80	99.54

Table 3. Cont.

Samples	XY-2	XY-2	XY-3	XY-3	XY-3
No.	1	2	6	7	8
Si	7.91	7.94	7.96	7.96	7.98
Al	0.04	0.06	0.04	0.04	0.02
Sum T	7.95	8.00	8.00	8.00	8.00
Al	0.00	0.00	0.00	0.00	0.03
Ti	0.00	0.00	0.00	0.00	0.00
Cr	0.00	0.00	0.00	0.00	0.00
Fe ³⁺	0.00	0.00	0.00	0.00	0.00
Zn	0.01	0.00	0.00	0.00	0.00
Mg	4.99	5.00	5.00	5.00	4.97
Ni	0.00	0.00	0.00	0.00	0.00
Fe ²⁺	0.00	0.00	0.00	0.00	0.00
Mn	0.00	0.00	0.00	0.00	0.00
Sum C	5.00	5.00	5.00	5.00	5.00
Mg	0.22	0.17	0.05	0.06	0.05
Ni	0.00	0.01	0.00	0.00	0.00
Fe ²⁺	0.02	0.03	0.03	0.03	0.05
Mn	0.00	0.00	0.01	0.00	0.00
Ca	1.76	1.79	1.84	1.85	1.79
Na	0.00	0.00	0.02	0.02	0.03
Sum B	2.00	2.00	1.95	1.96	1.92
Ca	0.10	0.01	0.00	0.00	0.00
Na	0.02	0.04	0.00	0.00	0.00
K	0.00	0.01	0.01	0.01	0.01
Sum A	0.12	0.06	0.01	0.01	0.01
F	0.00	0.00	0.16	0.13	0.14
OH	2.00	2.00	1.84	1.87	1.86
Sum W	2.00	2.00	2.00	2.00	2.00
Mg/(Mg + Fe ²⁺)	1.00	0.99	0.99	0.99	0.99
Mineral	Tr	Tr	Tr	Tr	Tr

Notes: Amphibole formulae were calculated on the basis of 23 oxygens to account for F and Cl replacing O. Fe³⁺ content was estimated based on the charge balance. Tr—tremolite. Measurements unit: Electron Probe Laboratory of the Institute of Science, CUGB.

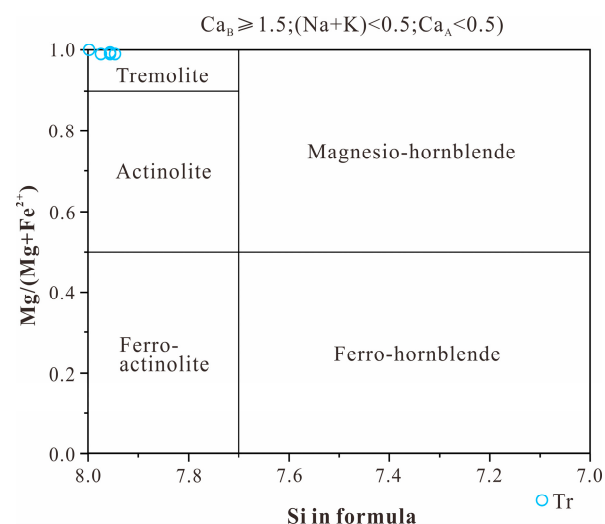


Figure 7. Amphibole classification in Xinyu nephrite. (Modified after [33]).

On the other hand, diopside is composed of (in wt.%) SiO₂ (54.91–55.16), CaO (23.75–24.02), MgO (18.66–18.97), and FeO_T (0.36–0.63). Fluorine was detected in some tremolite. Diopside grains are almost homogeneous and compositionally close to the diopside end-member (Table 4) [34]. Apatite in nephrite (Table 4) is composed of (in wt.%) CaO

(55.91–57.24) and P_2O_5 (40.21–40.68). Additionally, apatite is fluorine-enriched (0.82–0.84 a.p.f.u. F) and homogeneous. Calcite in nephrite (Table 5) is composed of (in wt.%) CaO (56.36–58.60) [35].

Table 4. Chemical composition of apatite and calcite in the Xinyu nephrite (wt.%).

Samples	XY-2	XY-2	XY-2	XY-3
No.	1	4	3	2
SiO ₂	54.91	55.16	0.14	0.09
TiO ₂	0.03	0.01	0.11	0.00
Al ₂ O ₃	0.13	0.15	0.00	0.00
Cr ₂ O ₃	0.02	0.01	0.01	0.01
FeO	0.63	0.36	0.07	0.00
MgO	18.66	18.97	0.01	0.02
ZnO	0.03	0.02	0.07	0.00
MnO	0.04	0.04	0.00	0.00
NiO	0.00	0.00	0.07	0.00
CaO	24.02	23.75	57.24	55.91
CuO	0.04	0.00	0.00	0.00
Na ₂ O	0.05	0.13	0.06	0.04
K ₂ O	0.01	0.00	0.02	0.02
P ₂ O ₅	0.00	0.00	40.21	40.68
SO ₃	0.01	0.04	0.03	0.01
F	0.00	0.00	3.16	3.21
Cl	0.00	0.00	0.04	0.02
Total	98.59	98.65	99.90	98.70
Si	2.00	2.01	0.01	0.01
Ti	0.00	0.00	0.01	0.00
Al	0.01	0.01	0.00	0.00
Cr	0.00	0.00	0.00	0.00
Fe ³⁺	0.00	0.00	0.00	0.00
Mg	1.02	1.03	0.00	0.00
Fe ²⁺	0.02	0.01	0.00	0.00
Zn	0.00	0.00	0.00	0.00
Mn	0.00	0.00	0.00	0.00
Ca	0.94	0.93	5.04	4.95
Cu	0.00	0.00	0.00	0.00
Na	0.00	0.01	0.01	0.01
K	0.00	0.00	0.00	0.00
P	0.00	0.00	2.80	2.84
S	0.00	0.00	0.00	0.00
F	0.00	0.00	0.82	0.84
Cl	0.00	0.00	0.01	0.00
Mineral	Di	Di	Ap	Ap

Note: The diopside formulae were calculated on the basis of 6 oxygens and the apatite formulae were calculated on the basis of 12.5 oxygens, respectively, to account for F and Cl replacing O. Fe³⁺ content was estimated according to the charge balance. Di—diopside; Ap—apatite. Measurements unit: Electron Probe Laboratory of the Institute of Science, CUGB.

Table 5. Chemical composition of calcite in the Xinyu nephrite (wt.%).

Samples	XY-2	XY-3	XY-3
No.	1	1	5
SiO ₂	0.05	0.16	0.02
Al ₂ O ₃	0.01	0.00	0.01
Cr ₂ O ₃	0.04	0.00	0.05
ZnO	0.09	0.07	0.00
MnO	0.00	0.05	0.02
NiO	0.00	0.04	0.09

Table 5. Cont.

Samples	XY-2	XY-3	XY-3
No.	1	1	5
MgO	0.15	0.02	0.01
CaO	58.60	56.36	57.21
CoO	0.00	0.07	0.00
CuO	0.04	0.08	0.04
Na ₂ O	0.05	0.05	0.02
SrO	0.00	0.33	0.09
Total	59.02	57.21	57.55
Minerals	Cal	Cal	Cal

Note: Cal—calcite. Measurements unit: Electron Probe Laboratory of the Institute of Science, CUGB.

4.4. Spectral Features

FTIR spectral features of tremolite in Xinyu nephrite are mainly reflected in three bands: 400–600 cm^{-1} , 600–800 cm^{-1} , and 900–1200 cm^{-1} (Figure 8). The absorption peaks near 416 cm^{-1} , 461 cm^{-1} , 510 cm^{-1} , and 542 cm^{-1} are attributed to Si-O bending vibration and M-O (M is Mg, Fe, and other metal cations) lattice vibrations [36,37]. The absorption peaks at 683 cm^{-1} and 758 cm^{-1} correspond to symmetric stretching vibrations of Si-O-Si bonds. The absorption peaks at 918 cm^{-1} , 996, and 1039 cm^{-1} are associated with asymmetric stretching vibrations of O-Si-O and Si-O-Si, as well as O-Si-O symmetric stretching vibration [37]. In addition, characteristic vibrational absorption peaks of other minerals were found in some samples, such as the CO_3^{2-} bending vibration of calcite at 876 cm^{-1} ; and the Si-O asymmetric stretching vibration of quartz at 1091 cm^{-1} , indicating the presence of other minerals. The band positions and assignments can be found in Table 6.

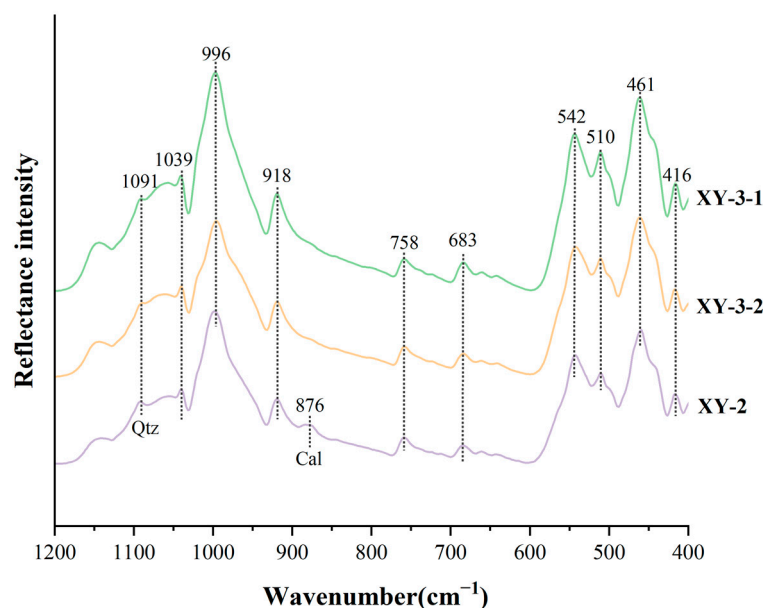


Figure 8. FTIR spectral features of Xinyu nephrite.

Raman spectral peaks in Xinyu nephrite are observed at 160 cm^{-1} , 179 cm^{-1} , 224 cm^{-1} , 395 cm^{-1} , 674 cm^{-1} , 930 cm^{-1} , and 1060 cm^{-1} (Figure 9, Table 7). Among them, the peaks at 160 cm^{-1} , 179 cm^{-1} , and 224 cm^{-1} are attributed to the lattice vibration of $[\text{SiO}_4]^{4-}$. The higher intensity of the peak at 674 cm^{-1} is associated with the symmetric stretching-bending vibration of Si-O-Si in the tetragonal ring composed of silica-oxygen tetrahedra [38]. The 1060 cm^{-1} peak is due to the ν_2 vibration of Si-O. These Raman spectral peaks reveal typical tremolite characteristics, similar to those of Xinjiang and Qinghai nephrite [14,39].

Table 6. FTIR band assignment of the Xinyu nephrite.

Wavenumbers (cm ⁻¹)	Band Assignment	Suggested Minerals
1039,996,918	O-Si-O and Si-O-Si asymmetric stretching vibration; O-Si-O symmetric stretching vibration	Tr
758,683	Si-O-Si symmetric stretching vibration	
542,510,461,416	Si-O bending vibration and M-O (M is Mg, Fe, and other metal cations) lattice vibrations	
1091	Si-O asymmetric stretching vibration	Qtz
876	CO ₃ ²⁻ bending vibration	Cal

Notes: Tr—tremolite; Qtz—quartz; Cal—calcite.

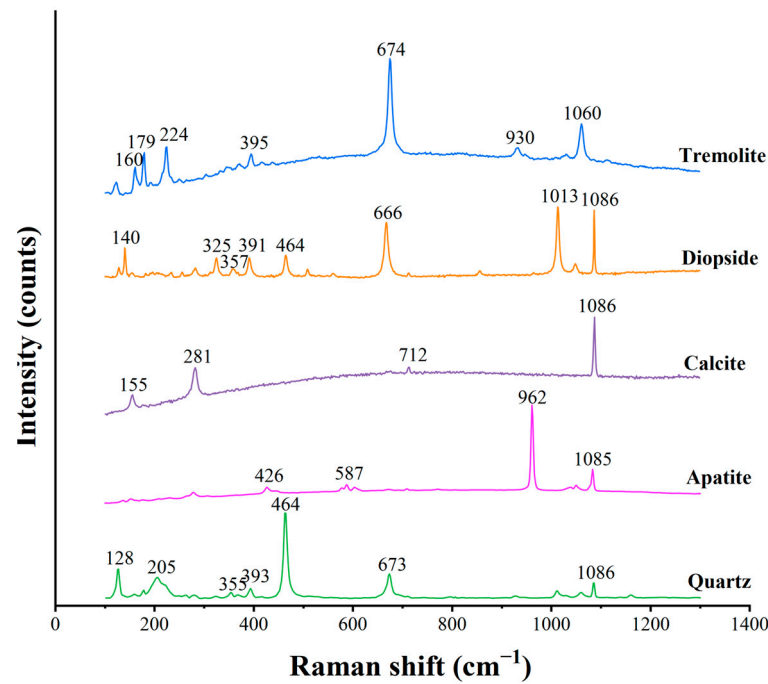


Figure 9. Laser Raman spectral features of Xinyu nephrite.

Table 7. Raman spectral peaks of the minerals in Xinyu nephrites.

Characteristic Raman Spectral Peaks	Suggested Minerals
160 cm ⁻¹ , 179 cm ⁻¹ , 224 cm ⁻¹ , 395 cm ⁻¹ , 674 cm ⁻¹ , 930 cm ⁻¹ , and 1 060 cm ⁻¹	Tr
140 cm ⁻¹ , 325 cm ⁻¹ , 357 cm ⁻¹ , 391 cm ⁻¹ , 666 cm ⁻¹ , 1013 cm ⁻¹	Di
155 cm ⁻¹ , 281 cm ⁻¹ , 712 cm ⁻¹ , and 1086 cm ⁻¹	Cal
426 cm ⁻¹ , 587 cm ⁻¹ , and 962 cm ⁻¹	Ap
128 cm ⁻¹ , 205 cm ⁻¹ , 355 cm ⁻¹ , and 464 cm ⁻¹	Qtz

Notes: Tr—tremolite; Di—diopside; Cal—calcite; Ap—apatite; Qtz—quartz.

Raman spectral features of diopside, calcite, apatite, and quartz were also examined (Figure 9, Table 7) and the results are consistent with those of EPMA. The Raman spectral peaks of diopside are mainly located at 140 cm⁻¹, 325 cm⁻¹, 357 cm⁻¹, 391 cm⁻¹, 666 cm⁻¹, and 1013 cm⁻¹. This is similar to the standard peak of diopside. The 1086 cm⁻¹ peak of calcite is also indicated in the spectral peak map of diopside. The Raman spectral peaks of calcite are located at 155 cm⁻¹, 281 cm⁻¹, 712 cm⁻¹, and 1086 cm⁻¹, and the test results do not show the peak test results of other minerals. The Raman spectral peaks of apatite were 426 cm⁻¹, 587 cm⁻¹, and 962 cm⁻¹, which were compatible with the standard values. The 1085 cm⁻¹ peak of calcite was also indicated in the Raman spectral of apatite. The Raman

spectral peaks of quartz were located at 128 cm^{-1} , 205 cm^{-1} , 355 cm^{-1} , and 464 cm^{-1} . In addition to this, small peaks with weaker intensities were also observed: 393 cm^{-1} , 673 cm^{-1} for tremolite, and 1086 cm^{-1} for calcite.

5. Discussion

5.1. Mineral Replacement Texture

As indicated by FTIR spectroscopy, Raman spectroscopy, and EPMA, the major minerals in Xinyu nephrite are tremolite, whereas the minor minerals include diopside, calcite, apatite, and quartz. These minerals exhibit mineral replacement texture.

The first and most common case in Xinyu nephrite is the replacement of diopside by tremolite. Fibrous tremolite grains can be observed growing along the boundary of the diopside, resulting in irregularly shaped diopside grains with an isolated island distribution (Figure 5c,e). Idiomorphic diopside grains are rare, only relics of diopside exist because of the incomplete metasomatism of tremolite replacement. Such replacement of diopside by tremolite has also been observed in nephrite from Qiemo, Xinjiang [40], Dahua, Guangxi [17], and Tieli, Heilongjiang [21]. Liu et al. [41] have reported the early formation of diopside and the replacement of diopside by tremolite.

Under the influence of the external environment, the diopside is metasomatized to tremolite. This metasomatic process results in the destruction of the diopside and the formation of uneven grain boundaries as tremolite replaces it (Figure 5e,f). However, due to incomplete metasomatism, the interior of the diopside was not completely replaced, retaining some of its original shape and resulting in an island-like appearance. As a result, the replacement of diopside by tremolite is a kind of common occurrence in nephrite, which helps to explain the rarity of idiomorphic diopside grains.

The second texture observed in Xinyu nephrite is the replacement of calcite by tremolite (Figure 5e). Calcite grains were replaced by tremolite both inside and in the surrounding area. Fibrous tremolite is observed at the edges of calcite, resulting in a replacement residual texture. The replacement and destruction of calcite grains can be seen in Figure 5e. Similar textures of calcite replacement have been reported in nephrite from a few other origins [42–44]. It has been reported [43,44] that calcite could be formed as a reactant during the diopside replacement process and is subsequently replaced by tremolite. Tremolite replaced calcite grains along fracture or other weak surfaces, resulting in the destruction of the original shape of calcite and leaving only part of calcite in a fragmented shape. The replacement of calcite confirms the existence of multiple phases of magmatic-hydrothermal events during the formation of nephrite.

The third texture is fine tremolite grains replacing coarse ones. Fine, randomly oriented tremolite fibers can be seen in the columnar tremolite grains (Figure 5b). The boundaries and shapes of fine grains cannot be discerned. During multiple mineral metasomatisms, the texture of tremolite became finer, resulting in a higher-quality of nephrite. This texture has been observed in various origins of high-quality nephrite [12,44].

Based on the replacement texture described above, the formation of tremolite can be characterized in three ways: (1) diopside transformation, (2) carbonate mineral transformation, and (3) coarse tremolite transformation. Currently, based on petrographic observations, the possible formation sequence of minerals in Xinyu nephrite is as follows: diopside was formed first, followed by coarse-grained tremolite, then fine-grained tremolite replaced both coarse-grained tremolite and diopside. Calcite, which is a reaction product of the diopside replacement process, was also replaced by tremolite in later hydrothermal events. Since tremolite is a hydrated silicate mineral, fluid-rock metasomatism played an important role in its formation, it is inferred that complete metasomatism could significantly improve the quality of nephrite.

5.2. Preliminary Discussion on the Genesis of Xinyu Nephrite

According to differences in geological background, nephrite deposits are generally reported to be divided into two types. One is related to dolomite (D-type) [2,9,12,21,40,43,45],

which forms by contact metasomatic replacement of dolomite marble by Si-rich aqueous fluids during the emplacement of a felsic pluton. The other is related to serpentinite (S-type) [2,7,46], which forms along fault contacts between serpentinite and mafic to felsic igneous rock or metagraywacke in obduction settings.

However, Xinyu nephrite is different from these two types. It appears in a contact zone between the Mengshan composite pluton and Permian carbonate rock. Petrographic studies suggest that the carbonate rock is a calcic marble that has undergone diopside and tremolite (Figure 6). No carbonate minerals have been observed in previous studies of the S-type nephrite. Minor minerals commonly found in S-type nephrites, such as spinel, chlorite, serpentine, chromite, magnetite [46–48], are not found in Xinyu nephrites. According to the above characteristics, we can speculate that Xinyu nephrite is not of S-type genesis. Due to its occurrence, strata is not composed of dolomite or dolomitic marble, but rather of limestone, which is different from the typical D-type nephrites reported so far. As the dominant mineral of the limestone is calcite, this atypical D-type genesis nephrite is essentially a calcite-replacement one, which we name C-type in this investigation.

Actually, C-type nephrites have been reported previously. For example, black nephrite from Dahua, Guangxi, is located at the boundary zone between diabase and limestone-bearing siliceous rock [49]; nephrite in Luodian, Guizhou was found to be produced in the contact metamorphic zone between basic diabase and calcic carbonate rock [50]. Recently, the white nephrite from the Mida deposit in Qiemo County, Xinjiang, was also reported to be related to limestone replacement [51]. These nephrites, including Xinyu nephrite, are all closely related to limestone, not dolomite.

The potential mechanism of Xinyu nephrite is postulated as follows: the intrusion of the Mengshan composite pluton into silica-calcium-magnesium-rich limestone provided the mineralization source, with the heat generated by the intruded body of the Mengshan pluton. These factors facilitate the formation of nephrite. Further research is required to fully comprehend its mechanism. As a new C-type one, the discovery of Xinyu nephrite occurrence would call for more attention, and emphasis would be paid on the Ca-skarn type in looking for new nephrite deposits.

5.3. Gemological Significance

The discovery of new origins is urgent due to the increasing exploitation of nephrite resources. There have been no reports of any jade appearing in Jiangxi Province, let alone gem-quality nephrite jade. Thus, our first report in this province has great gemological significance.

The color of Xinyu nephrite is a light yellow-green, which is relatively rare in nephrite of other regions. Compared with previously reported nephrites from Xinjiang and Qinghai in China, as well as nephrites from South Korea and Russia [16,44,52,53], it was observed that Xinyu nephrite also exhibited a relatively uniform color. The uniform and beautiful color indicates that Xinyu nephrite has a high value as a gemstone.

Gemological tests indicate that Xinyu nephrite exhibits a refractive index of 1.60–1.61, a relative density of 2.90–2.91, and a Mohs hardness of 5.78–5.83. These results align with the National Standard of China GB/T 38821-2020 [54]. Generally, the finer the tremolite grains, the better the quality of nephrite. In Xinyu nephrite, SEM analysis and petrographic observations have revealed a large number of fibrous tremolite grains with a fine texture. The texture characteristics of tremolite contribute to the high toughness of Xinyu nephrite, which makes it show a great greasy luster on the surface.

6. Conclusions

In this study, we reported a new nephrite occurrence in Xinyu County, Jiangxi Province for the first time. Nephrite exhibits a light yellow-green color, is slightly-translucent to translucent, and has a medium-greasy luster. It mainly comprises tremolite, with minor amounts of diopside, calcite, quartz, and apatite. Gemological and spectroscopic studies show that Xinyu nephrite meets the criteria for gem-quality nephrite.

Metasomatism in Xinyu nephrite prevails, mainly in the form of diopside, calcite, and coarse tremolite replacement by fine tremolite. The diopside is encompassed by fibrous tremolites, forming an island-style microstructure. The replaced calcite shows a residual texture, and the fine tremolite fibers are randomly oriented and tightly distributed. These distinct replacement patterns offer valuable insights into the mineralization process of Xinyu nephrite, meriting further investigation.

Xinyu nephrite occurs in a contact zone between the Mengshan granitic pluton and Permian limestones. The formation process is related to calcic marble that underwent diopsidization and tremolitization, which differs from the two classically reported types (D-type: dolomite-related; S-type: serpentinite-related). As a newly identified C-type occurrence, the discovery of Xinyu nephrite demands heightened attention, specifically directing focus towards the Ca-skarn type for the discovery of new nephrite deposits.

Author Contributions: Conceptualization, X.W. and G.S.; methodology, X.W. and G.S.; software, X.W.; validation, X.W., G.S., X.Z. and M.S.; formal analysis, X.W., G.S. and X.Z.; investigation, X.W., G.S., X.Z., J.Z. and M.S.; resources, J.Z.; data curation, X.W. and G.S.; writing—original draft preparation, X.W. and G.S.; writing—review and editing, G.S., X.Z. and M.S.; visualization, X.W.; supervision, G.S.; project administration, G.S.; funding acquisition, G.S. and J.Z. All authors have read and agreed to the published version of the manuscript.

Funding: This research was funded by the National Science Foundation of China (Grant No. 42273044).

Data Availability Statement: The data presented in this study are available in this article.

Acknowledgments: We gratefully appreciate Liu, T.Z. (Basic Geological Survey Institute of Jiangxi Geological Survey and Exploration Institute) for the kind support during the field investigation, Zhang, Y., Li, Y.H., Wen, J.B. and Deng, Q.Q., at CUGB for their analytic support. Constructive and thoughtful comments from three anonymous reviews and comments, along with editorial handling by journal editors are gratefully appreciated.

Conflicts of Interest: The authors declare no conflicts of interest.

References

1. Wang, R. Progress Review of the Scientific Study of Chinese Ancient Jade. *Archaeometry* **2011**, *53*, 674–692. [[CrossRef](#)]
2. Harlow, G.E.; Sorensen, S.S. Jade (Nephrite and Jadeitite) and Serpentinite: Metasomatic connections. *Int. Geol. Rev.* **2005**, *47*, 113–146. [[CrossRef](#)]
3. Chen, T.H.; Calligaro, T.; Pages-Camagna, S.; Menu, M. Investigation of Chinese archaic jade by PIXE and mu Raman spectrometry. *Appl. Phys. A Mater. Sci. Process.* **2004**, *79*, 177–180. [[CrossRef](#)]
4. Tsydenova, N. Chemical and spectroscopic study of nephrite artifacts from Transbaikalia, Russia: Geological sources and possible transportation routes. *Quat. Int.* **2015**, *355*, 114–125. [[CrossRef](#)]
5. Sui, J.; Liu, X.; Guo, S. Spectrum Research of Nephrite From Qinghai and South Korea. *Laser Optoelectron. Prog.* **2014**, *51*, 73002. [[CrossRef](#)]
6. Feng, Y.; He, X.; Jing, Y. A new model for the formation of nephrite deposits: A case study of the Chuncheon nephrite deposit, South Korea. *Ore Geol. Rev.* **2022**, *141*, 104655. [[CrossRef](#)]
7. Jiang, B.; Bai, F.; Zhao, J. Mineralogical and geochemical characteristics of green nephrite from Kutcho, northern British Columbia, Canada. *Lithos* **2021**, *388*, 106030. [[CrossRef](#)]
8. Liao, G.; Yang, X.; Jing, C.; Zhou, Z.; Jin, X. Mineral Composition and Chemical Composition Characteristics of Green Nephrite from Three Origins. *J. Tongji Univ. Nat. Sci.* **2022**, *50*, 1110–1114. [[CrossRef](#)]
9. Shi, G.; Jia, R.; Santosh, M.; Liang, H.; He, H. First report of a nephrite deposit from Somaliland, Africa: Characterization and geological and archaeological implications. *GSA Bull.* **2024**, *136*, 661–672. [[CrossRef](#)]
10. Zhao, H.; Gan, F. Application of Raman Spectroscopic Technique to the Identification and Investigation of Chinese Ancient Jades and Jade Artifacts. *Spectrosc. Spectr. Anal.* **2009**, *29*, 2989–2993. [[CrossRef](#)]
11. Fu, X.; Gan, F.; Ma, B.; Gu, D. Structural and nondestructive componential analysis on several Nephrite from different provenances. *Acta Petrol. Sin.* **2007**, *23*, 1197–1202, (In Chinese with English Abstract).
12. Zhang, X.; Shi, G.; Zhang, X.; Gao, K. Formation of the Nephrite Deposit with Five Mineral Assemblage Zones in the Central Western Kunlun Mountains, China. *J. Petrol.* **2022**, *63*, egac117. [[CrossRef](#)]
13. Han, D.; Liu, X.; Liu, Y.; Zhang, Y.; Zheng, F.; Maituohuti, A.; Zhang, H.; Wen, Z. Genesis of dolomite-related nephrite from Hetian and color-forming factors of typical nephrite in Hetian, Xinjiang. *Acta Petrol. Mineral.* **2018**, *37*, 1011–1026.
14. Zhang, Y.; Liu, Y.; Liu, T.; Zari, M.; Liu, Y.-Q. Vibrational Spectra of Hetian Nephrite from Xinjiang. *Spectrosc. Spectr. Anal.* **2012**, *32*, 398–401.

15. Zhou, Z.; Liao, Z.; Chen, Y.; Yujia, L.; Tingting, M. Petrological and Mineralogical Characteristics of Qinghai Nephrite. *Rock Miner. Anal.* **2008**, *27*, 17–20. (In Chinese with English Abstract)
16. Yu, H.; Ruan, Q.; Sun, Y.; Li, D. Micro-morphology and Mineral Composition of Different Color Qinghai Nephrites. *Rock Miner. Anal.* **2018**, *37*, 626–636.
17. Bai, F.; Du, J.; Li, J.; Jiang, B. Mineralogy, geochemistry, and petrogenesis of green nephrite from Dahua, Guangxi, Southern China. *Ore Geol. Rev.* **2020**, *118*, 103362. [[CrossRef](#)]
18. Zheng, F.; Liu, Y.; Zhang, H. The Petrogeochemistry and Zircon U—Pb Age of Nephrite Placer Deposit in Xiuyan, Liaoning. *Rock Miner. Anal.* **2019**, *38*, 438–448.
19. Zhang, Y.; Qiu, Z.; Peng, S.; Zhong, Y.; Li, L.; Wu, M. The Genesis of Graphites in Xiuyan Gravel Nephrite Jades and Its Constraint on Their Host Nephrite Jade Rocks. *Acta Sci. Nat. Univ. Sunyatseni* **2015**, *54*, 118–126. [[CrossRef](#)]
20. Bai, F.; Li, G.; Lei, J.; Sun, J. Mineralogy, geochemistry, and petrogenesis of nephrite from Panshi, Jilin, Northeast China. *Ore Geol. Rev.* **2019**, *115*, 103171. [[CrossRef](#)]
21. Gao, S.; Bai, F.; Heide, G. Mineralogy, geochemistry and petrogenesis of nephrite from Tieli, China. *Ore Geol. Rev.* **2019**, *107*, 155–171. [[CrossRef](#)]
22. Li, H.; Zuo, D. Geological Characteristics and Genesis Analysis of Diopside Deposit in Southeastern Mengshan, Jiangxi. *Mod. Min.* **2022**, *38*, 71–74. (In Chinese with English Abstract)
23. Wang, X.; Hu, Z.; Yu, X.; Chen, G.; Li, Y.; Zhan, T.; Chen, S.; Liu, S.; Cheng, X.; Yang, S. Geological Characteristics and Prospecting Significance of the Shizhushan Superlarge Wollastonite Deposit in Mengshan, West Jiangxi Province. *Acta Geosci. Sin.* **2019**, *40*, 259–264.
24. Shu, L.; Faure, M.; Wang, B.; Zhou, X.; Song, B. Late Palaeozoic-Early Mesozoic geological features of South China: Response to the Indosinian collision events in Southeast Asia. *Comptes Rendus Geosci.* **2008**, *340*, 151–165. [[CrossRef](#)]
25. Mu, J.; Zhao, S.; Brzozowski, M.; Li, H.; Wu, C.; Li, W. Geology, geochemistry and genesis of the world-class Shizhushan wollastonite deposit, Mengshan area, South China. *Ore Geol. Rev.* **2023**, *158*, 105469. [[CrossRef](#)]
26. Yang, Y.; Pan, X.; Hou, Z.; Deng, Y.; Ouyang, Y.; Meng, D.; Xie, T. Petrogenesis, Redox State, and Mineralization Potential of Triassic Granitoids in the Mengshan District, South China. *Front. Earth Sci.* **2021**, *9*, 657618. [[CrossRef](#)]
27. Hu, Z. *The Formation Conditions and Metallogenic Regularity of Zhuxi Tungsten Polymetallic Deposit in Northeast of Jiangxi Province*; Chengdu University of Technology: Chengdu, China, 2016. (In Chinese with English Abstract)
28. Zhong, Y.; Ma, C.; She, Z.; Xu, H.; Wang, S.; Wang, L. U-Pb-Hf Isotope of Zircons, Geochemistry and Genesis of Mengshan Granitoids in Northwestern Jiangxi Province. *Earth Sci.* **2011**, *36*, 703–720.
29. Liao, M. Geological Characteristics and Genesis of Non-Metallic and Polymetallic Deposits of Mengshan Region, Jiangxi Province. *Adv. Geosci.* **2012**, *2*, 211–216. [[CrossRef](#)]
30. Mao, J.; Cheng, Y.; Chen, M.; Pirajno, F. Major types and time-space distribution of Mesozoic ore deposits in South China and their geodynamic settings. *Miner. Depos.* **2013**, *48*, 267–294. [[CrossRef](#)]
31. Zhang, Y.; Shao, Y.; Liu, Q.; Chen, H.; Quan, W.; Sun, A. Jurassic magmatism and metallogeny in the eastern Qin-Hang Metallogenic Belt, SE China: An example from the Yongping Cu deposit. *J. Geochem. Explor.* **2018**, *186*, 281–297. [[CrossRef](#)]
32. Wang, S.Q.; Shi, G.H. *Nephrite from Xinjiang, China, Volume 1*; Science Press: Beijing, China, 2022.
33. Leake, B.E. Nomenclature of amphiboles—Report of the subcommittee on Amphiboles of the International Mineralogical Association Commission on New Minerals and Mineral Names. *Eur. J. Mineral.* **1997**, *9*, 623–651. [[CrossRef](#)]
34. Morimoto, N.; Fabries, J.; Ferguson, A.K.; Ginzburg, I.V.; Ross, M.; Seifert, F.A.; Zussman, J.; Aoki, K.; Gottardi, G. Nomenclature of Pyroxenes. *American Mineralogist* **1988**, *73*, 1123–1133.
35. Hawthorne, F.C.; Oberti, R.; Harlow, G.E.; Maresch, W.V.; Martin, R.F.; Schumacher, J.C.; Welch, M.D. Nomenclature of the amphibole supergroup. *Am. Mineral.* **2012**, *97*, 2031–2048. [[CrossRef](#)]
36. Wen, L.; Liang, W.; Zhang, Z.; Huang, J. *Infrared Spectroscopy of Minerals*; Chongqing University Press: Chongqing, China, 1989.
37. Zhi, Y.; Liao, Z.; Zhou, Z.; Zhao, B.; Wang, B. A Resolution to the Hydroxy Types of Nephrite and Its Near Infrared Spectroscopy. *Spectrosc. Spectr. Anal.* **2013**, *33*, 1481–1486. [[CrossRef](#)]
38. Li, K.; Shen, X. Research on Identification Characteristics of Tremolite and Actinolite by Using Nondestructive Testing Techniques of Infrared Spectroscopy and Raman Spectroscopy. *Bull. Mineral. Petrol. Geochem.* **2019**, *38*, 405–408+427. [[CrossRef](#)]
39. Quanli, C.; Yalan, X.; Sujie, A.; Anqi, H.; Zuowei, Y. Vibrational Spectra of Caesious Nephrite form Qinghai Province. *Spectrosc. Spectr. Anal.* **2014**, *34*, 2017–2020. (In Chinese with English Abstract)
40. Liu, X.; Jia, Y.; Liu, Y. Geochemical Characteristics and Genetic Types of Gobi Nephrite in RuoqiangQiemo, Xinjiang. *Rock Miner. Anal.* **2019**, *38*, 316–325. [[CrossRef](#)]
41. Liu, Y.; Zhang, R.; Zhang, Z.; Shi, G.; Zhang, Q.; Abuduwayiti, M.; Liu, J. Mineral inclusions and SHRIMP U-Pb dating of zircons from the Alamas nephrite and granodiorite: Implications for the genesis of a magnesian skarn deposit. *Lithos* **2015**, *212*, 128–144. [[CrossRef](#)]
42. Li, N.; Bai, F.; Peng, Q.; Liu, M. Geochemical Characteristics of Nephrite from Chuncheon, South Korea: Implications for Geographic Origin Determination of Nephrite from Dolomite-Related Deposits. *Crystals* **2023**, *13*, 1468. [[CrossRef](#)]
43. Liu, Y.; Deng, J.; Shi, G.; Sun, X.; Yang, L. Geochemistry and petrogenesis of placer nephrite from Hetian, Xinjiang, Northwest China. *Ore Geol. Rev.* **2011**, *41*, 122–132. [[CrossRef](#)]

44. Jiang, Y.; Shi, G.; Xu, L.; Li, X. Mineralogy and Geochemistry of Nephrite Jade from Yinggelike Deposit, Altyn Tagh (Xinjiang, NW China). *Minerals* **2020**, *10*, 418. [[CrossRef](#)]
45. Liu, Y.; Deng, J.; Shi, G.; Yui, T.; Zhang, G.; Abuduwayiti, M.; Yang, L.; Sun, X. Geochemistry and petrology of nephrite from Alamas, Xinjiang, NW China. *J. Asian Earth Sci.* **2011**, *42*, 440–451. [[CrossRef](#)]
46. Gil, G.; Baginski, B.; Gunia, P.; Madej, S.; Sachanbinski, M.; Jokubauskas, P.; Belka, Z. Comparative Fe and Sr isotope study of nephrite deposits hosted in dolomitic marbles and serpentinites from the Sudetes, SW Poland: Implications for Fe-As-Au-bearing skarn formation and post-obduction evolution of the oceanic lithosphere. *Ore Geol. Rev.* **2020**, *118*, 103335. [[CrossRef](#)]
47. Korybska-Sadlo, I.; Gil, G.; Gunia, P.; Horszowski, M.; Sitarz, M. Raman and FTIR spectra of nephrites from the Zloty Stok and Jordanow Slaski (the Sudetes and Fore-Sudetic Block, SW Poland). *J. Mol. Struct.* **2018**, *1166*, 40–47. [[CrossRef](#)]
48. He, W.; Bai, F.; Zhao, C.; Qu, H.; Li, X. Petrogenesis of Chatoyant Green Nephrite from Serpentinite-Related Deposits, Ospinsk, Russia: Insights from Mineralogy and Geochemistry. *Crystals* **2023**, *13*, 252. [[CrossRef](#)]
49. Zhong, Q.; Liao, Z.; Qi, L.; Zhou, Z. Black Nephrite Jade from Guangxi, Southern China. *Gems Gemol.* **2019**, *55*, 198–215. [[CrossRef](#)]
50. Yang, L.; Lin, J.; Wang, L.; Tan, J.; Wang, B. Petrochemical characteristics and genetic significance of Luodian jade from Guizhou. *J. Mineral. Petrol.* **2012**, *32*, 12–19.
51. Jiang, T.; Shi, G.; Ye, D.; Zhang, X.; Zhang, L.; Han, H. A New Type of White Nephrite from Limestone Replacement along the Kunlun–Altyn Tagh Mountains: A Case from the Mida Deposit, Qiemo County, Xinjiang, China. *Crystals* **2023**, *13*, 1677. [[CrossRef](#)]
52. Liu, Y.; Deng, J.; Shi, G.; Lu, T.; He, H.; Ng, Y.; Shen, C.; Yang, L.; Wang, Q. Chemical Zone of Nephrite in Alamas, Xinjiang, China. *Resour. Geol.* **2010**, *60*, 249–259. [[CrossRef](#)]
53. Wilkins, C.J.; Tennant, W.C.; Williamson, B.E.; McCammon, C.A. Spectroscopic and related evidence on the coloring and constitution of New Zealand jade. *Am. Mineral.* **2003**, *88*, 1336–1344. [[CrossRef](#)]
54. GB/T 38821-2020; Hetian Yu—Testing and Classification. National Standard of the People’s Republic of China: Beijing, China, 2020. (In Chinese)

Disclaimer/Publisher’s Note: The statements, opinions and data contained in all publications are solely those of the individual author(s) and contributor(s) and not of MDPI and/or the editor(s). MDPI and/or the editor(s) disclaim responsibility for any injury to people or property resulting from any ideas, methods, instructions or products referred to in the content.